Identifying salt stratifications performing the machine learning approach over seismic attributes

Flavio Costa de Mesquita(GISIS/UFF), Marco Antonio Cetale Santos(GISIS/UFF), Alexandre Rodrigo Maul(Petrobras/UFF) and Alex Laier Bordignon(UFF)

Abstract

To build a seismic image we need to process the information from rock interfaces reflections. These reflections occurs as function of the impedance properties differences among the rocks, which is calculated as a combination of density and compressional velocity (inverse of slowness) measurements. Halite, usually the most abundant mineral on the section so-called salt, has an average density about 2,14 g/cm3 and compressional velocity in the order of 4,500 m/s. In terms of seismic studies, until the extreme recent time, the evaporite section was considered to be approximately constant, and reflecting the properties of halite. However, with the evolution of seismic migration algorithms and the computational capacity, it was perceived the need to make the salt section less homogeneous, since the evaporites formation (the evaporation process) occurs in stages, according to specific evaporation rates , generating the observed layering, still also denominated as stratifications, "enigmatic" reflectors/structures. In order to overcome this problem, we need better-elaborated velocity models that take into account these stratifications. In this work we used images of seismic sections and two types of seismic attributes, which will serve as input for a selected Machine Learning algorithm. Thereby allowing identifying from these 2D sections the stratifications within the salt layer allowing the characterization of the corresponding salt type.

Introduction

The field-reservoir under study is located in the central portion of the Santos Basin, about 180 km off the coast of the municipality of Rio de Janeiro in a water depth of approximately 1,900 m depth. The reservoirs of this field are situated between 5,000 and 6,000 m below the sea level and under a layer of salt, the Ariri Formation, which can range from a few hundred meters to over 2,000 m. We do know that this formation is not a homogeneous one, and that it is composed of different types of stratified minerals, the (evaporites). Usually, in the exploratory wells, the log registering of this layer of evaporites is carried out because these are "unknown" areas. In development wells, in general, the logs are no longer acquired within this layer mainly because the project economy. Depending on the complexity of the field and the saline structuring, there are variations in these "strata" and in their thickness, Oliveira et al. (2015), indicated an inverse correlation between "salt thickness" and "salt velocity variation". There are many types of evaporite minerals within the evaporitic section in the Santos and Campos basins, the most common being halite, anhydrite, gypsum, carnallite, tachyhydrite, sylvite. Studies carried out in log analysis show that not all these types of minerals will be seismically detectable by amplitude (Gobatto et al., 2016). Thus, to facilitate the strata identification, the evaporitic minerals in the salt section were grouped into three major facies: halite, high velocity salts (anhydrite and gypsite) and low velocity salts (carnallite, sylvite and tachyhydrite) as per emphasized in Maul et al.(2018). Table 1 presents the mineral grouping as proposed by Maul et al. (2018), indicating the chemical formula of each mineral as well as their acoustic properties.

GROUP	MINERAL	COMPOSITION	DENSITY (g/cm3)	COMPRESSIONAL VELOCITY (m/s)
LVS	Tachyhydrite Carnallite Sylvite	CaMg2Cl6.12(H2O) KMgCl3.6(H2O) KCl	1.57 1.66 1.86	3,300 3,910 3,910
BACKGROUND	Halite	NaCl	2.10	4,550
HVS	Gypsum Anhydrite	CaSO4.2(H2O) CaSO4	2.35 2.98	5,810 6,100

Table 1: Mineral groups and respective properties, average values compiled by Maul et al. (2018) covering more than 200 well in Santos Basin. Low Velocity Salts (LVS), Halite (Background) and High Velocity Salts (HVS).

Maul et al. (2018) based on the methodology proposed by Amaral et al. (2015), compiled the information from more than 200 wells in Santos Basin, showing the halite predominance, over 80% of occurrence. This percentage explains why it is considered as the background class and the main reason the seismic processing starts from the halite velocity property for the entire salt section at the tasks the velocity is needed. The remaining 20% of mineral occurrence can be split as:

- Anhydrite, gypsum, with high values of density and compressional velocity (compared to Halite), facies with low solubility. The basal Anhydrite represents the main seal of reservoirs in the Santos Basin.
- Tachyhydrite, carnallite, and sylvite, whose densities and compressional velocities are smaller than the

groups described above. They are also more soluble, a factor that makes drilling wells more difficult in this basin.

- Other studies also considered halite, the background mineral in this section, representing 75-90% of occurrences (Yamamoto et al., 2016, Gobatto et al., 2016).The proportion of salt varies for each well and its magnitude is related to the geological conditions where the well was drilled. In the ”salt walls” Halite normally represents more than 90% and in the mini basins the proportion of salt with high and low velocities varies between 10 and 20% each, consequently decreasing the halite content.

These differences in density and compressional velocity create the clear reflections within the ”saline section”. These seismic responses have received several denominations, such as: Enigmatic Reflector (Mohriak et al., 2004); Enigmatic Structure (Jackson et al., 2015); Stratification (Maul et al., 2015)). Ji et al. (2011) already indicates that even the insertion of randomly heterogeneities into the salt (the so-called ”dirty salt”) already assists in the production of better seismic images by their selected migration algorithms.

Materials and Methods

To date, Machine Learning has been used in the seismic scale to predict geological structures, stratigraphy, and rock and fluid properties, usually through seismic interpretation and inversion. In order to do so, fully convolutional deep networks have been used in the area of fault interpretation (Long et al., 2015), 3D convolutional neural networks (Waldeland et al., 2018) and deep encoder-decoder networks for stratigraphic interpretation (Badrinarayanan et al., 2015). These techniques classify a 3D Post-Stack data set based on 3D sub-cubes or 2D sections, and require a relatively low number of labels. Interpretation in seismic images has long used texture attributes to better identify and highlight areas of interest. These can be seen as feature maps in seismic texture. For salt, it can be noted that the texture in the salt masks are quite chaotic, where the surrounding seismic is more ”striped”. However this is not always true, as we can see in the Santos Basin, where the salt layer is highly stratified.

In this work we use an unsupervised classification algorithm, where the classes we wish to find are the 3 evaporite groups, according to the nomenclature mentioned in Maul et al., (2018): LVS, Halite and HVS.

The seismic data used here is a piece of a Pre-Stack Depth Migration type (PSDM). From this data was extracted an ***in-line*** in SEG-Y and the amplitude response was used as one of the inputs of the algorithm.

Another seismic attribute used was the Relative Acoustic Impedance (RAI), which is a good seismic attribute for the quantitative analysis of beddings (especially in thin strata such as in our case), due to its low amount of low frequency content. Samples with lower seismic amplitude have RAI values related to LVS; samples with higher seismic amplitude have RAI values related to HVS; the remainder can be characterized as halite. To calculate the attribute we use the amplitude response in the extracted ***in-line*** and used as the second input for the algorithm.

The third seismic attribute entry was the TECVA (Amplitudes Volume Technique) type. This attribute aims at the generation of amplitude maps and vertical and horizontal seismic sections that reflect, as far as possible, subsurface geology. Where the knowledge of geology is very dependent on seismic information, it is necessary the details of imaging at the boundaries between the seismic sequences or their inner layers (Bulhões and Amorim, 2005). The Elementary SeismoLayer is the rock layer of smaller thickness that the seismic data can solve and it is defined as the key element of weighting for the calculation and obtaining of the seismic data with the TECVA.

In our case the salt stratifications can be of the magnitude of only a few meters, way below the seismic resolution. Therefore, we need seismic attributes that focus on the high frequencies such as RAI and TECVA combined, in order to better define the stratifications within the salt. A comparison of the three can be seen in figure 1.

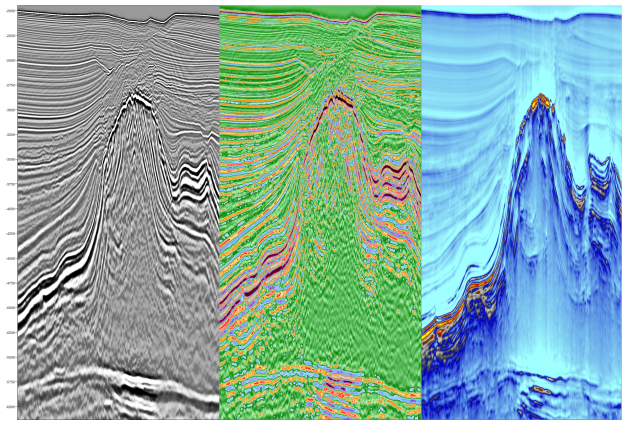

Figure 1: Images used as input: on the left, seismic amplitude section; on the center, relative acoustic impedance; on the right, the TECVA.

Clusterizing

In our case, because it is an image with many features, we used an unsupervised classification that separates the pixels by classes in clusters, for this a sliding window was used on the image as in figure 2, as per defended by Yang et al. (2016).

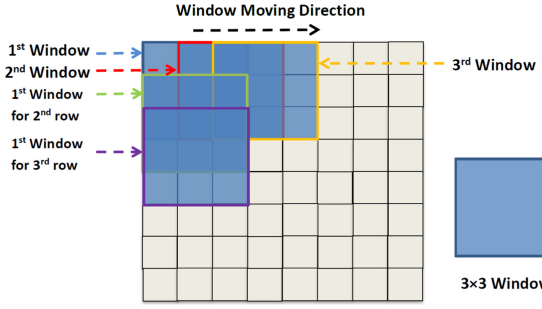

Figure 2: Sliding window. Source: Yang et al. (2016).

For the clusters classification , we use the algorithm t-SNE (van der Maaten and Hinton, 2008). It is a nonlinear dimensionality reduction technique suitable for use with

high-dimensional data for visualization in a small space, as two or three dimensions. Specifically, it models each high-dimensional object by a two-dimensional or three-dimensional point such that similar objects are modeled by nearby points and distant points model different objects with high probability. The resulting clustering can be seen in figure 3.

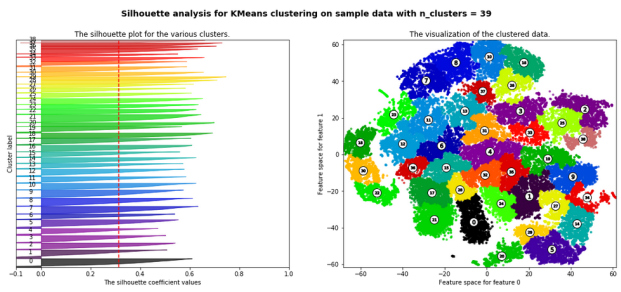

Figure 3: Pixels classified into clusters, each representing a class found in the input images

t-SNE is based on probability distributions with random walk in neighborhood graphs to find the structure within the data. Given a set of *N* high-dimensional objects $\mathbf{x}_1, ..., \mathbf{x}_N$, t-SNE first computes probabilities p_{ij} that are proportional to the similarity of objects $\mathbf{x}_i$ and $\mathbf{x}_j$, as follows:

$$p_{j|i} = \frac{\exp(-\mathbf{x}_i - \mathbf{x}_j^2/2\sigma_i^2)}{\sum_{k \neq i} \exp(-\mathbf{x}_i - \mathbf{x}_k^2/2\sigma_i^2)}, \tag{1}$$

As van der Maaten and Hinton (2008) explained: "The similarity of datapoint $x_j x_j$ to datapoint x_i is the conditional probability, $p_{j|i}$, that x_i would pick x_j as its neighbor if neighbors were picked in proportion to their probability density under a Gaussian centered at x_i."

$$p_{ij} = \frac{p_{j|i} + p_{i|j}}{2N} \tag{2}$$

Moreover, the probabilities with *i = j* are set to zero : $p_{ij} = 0$

The bandwidth of the Gaussian kernels σ_i, is set in such a way that the perplexity of the conditional distribution equals a predefined perplexity using the bisection method. As a result, the bandwidth is adapted to the density of the data: smaller values of σ_i are used in denser parts of the data space.

Since the Gaussian kernel uses the Euclidean distance $x_i - x_j$, it is affected by the curse of dimensionality, and in high dimensional data when distances lose the ability to discriminate, the p_{ij} become too similar (asymptotically, they would converge to a constant). Schubert and Gertz (2017) proposed to adjust the distances with a power transform, based on the intrinsic dimension of each point, to alleviate this.

t-SNE aims to learn a *d*-dimensional map $y_1, \ldots, y_N$ (with $y_i \in R^d$) that reflects the similarities p_{ij} as well as possible. To this end, it measures similarities q_{ij} between two points in the map y_i and y_j, using a very similar approach. Specifically, q_{ij} is defined as:

$$q_{ij} = \frac{(1 + \mathbf{y}_i - \mathbf{y}_j^2)^{-1}}{\sum_{k \neq l} (1 + \mathbf{y}_k - \mathbf{y}_l^2)^{-1}} \tag{3}$$

Herein a heavy-tailed Student's t-distribution (with one-degree of freedom, which is the same as a Cauchy distribution) is used to measure similarities between low-dimensional points in order to allow dissimilar objects to be modeled far apart in the map. Note that also in this case we set $q_{ii} = 0$.

The locations of the points y_i in the map are determined by minimizing the (non-symmetric) Kullback–Leibler divergence of the distribution *Q* from the distribution *P*, that is:

$$KL(P||Q) = \sum_{i \neq j} p_{ij} \log \frac{p_{ij}}{q_{ij}} \tag{4}$$

The minimization of the Kullback–Leibler divergence with respect to the points y_i is performed using descending gradient. The result of this optimization is a map that reflects the similarities between the high-dimensional inputs.

Classifying

After finding all of the classes for the input images in separate clusters, we saved the resulting cluster labels. Then we train a classifier using these labels as a target variable and use it for classifying a new image. At this classification, we use two methods, K-Means centers and cKDTree in order to compare.

- *K-Means classification is a method of vector quantization,it aims to partition n observations into k clusters in which each observation belongs to the cluster with the nearest mean, serving as a prototype of the cluster. This results in a partitioning of the data space into Voronoi cells. The center points are vectors of the same length as each data point vector and are the "X's" in figure 3. Each data point is classified by computing the distance between that point and each group center, and then classifying the point to be in the group whose center is closest to it.*

- *cKDTree provides an index into a set of k-dimensional points which can be used to rapidly look up the nearest neighbors of any point.The used algorithm is described in Maneewongvatana and Mount (1999). The general idea is that the KDTree is a binary tree in which every leaf node is a k-dimensional point. Every non-leaf node can be thought of as implicitly generating a splitting hyperplane that divides the space into two parts, known as half-spaces. Points to the left of this hyperplane are represented by the left subtree of that node and points to the right of the hyperplane are represented by the right subtree. The hyperplane direction is chosen in the following way: every node in the tree is associated with one of the k dimensions, with the hyperplane perpendicular to that dimension's axis. So, if for a particular split the "x" axis is chosen, all points in the subtree with a smaller "x" value than the node will appear in the left subtree and all points with larger "x" value will be in the right subtree. In such a case, the hyperplane would be set by the x-value of the point, and its normal would be the unit x-axis, (Bentley, 1975).*

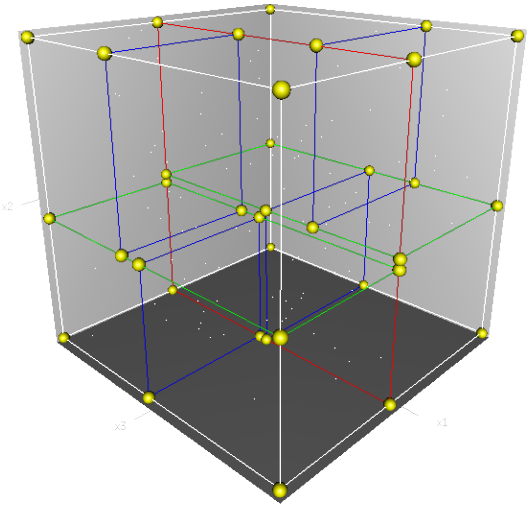

Figure 4: A 3-dimensional cKDTree. The first split (the red vertical plane) cuts the root cell (white) into two subcells, each of which is then split (by the green horizontal planes) into two subcells. Finally, four cells are split (by the four blue vertical planes) into two subcells. Since there is no more splitting, the final eight are called leaf cells. Source: http://www.stat.purdue.edu/ btyner/packages.html

Results

From what we could observe until this stage of this research, the t-SNE algorithm is the proper one for this kind of work, which involves the information clusterization, better identifying the image features in a timely manner and a small error of only 2.66% after 1,000 iterations. From that, we used the cluster labels generated to classify another image with two different algorithms, K-Means and cKDTree.

When we compare the resultant images, we clearly can see that cKDTRee was better to classify the image not only on the salt region but also in its surrounds. As we can see on figure 5 (a) a thinly laminated sequence outside the salt, inside the black circle, posed a challenge to imaging. It is due to the low seismic resolution, which is limited to 25 m, causing the image to be blurred and with small definition on this region. Beyond this, some parts of the salt tend to show a homogeneous behavior, as shown inside the red circle.

After using the K-Means classification, figure 5 (b) it had a small improvement. However, it still showed that blurred behavior of the original image.

When we used the cKDTree classifier, figure 5 (c), we could finally see some features we could not see before, on the original image. Some regions of the salt started to present a clear stratification showing different classes, colors, where it was previously more homogeneous . The blurred region outside the salt started to show the laminations we could not see before.

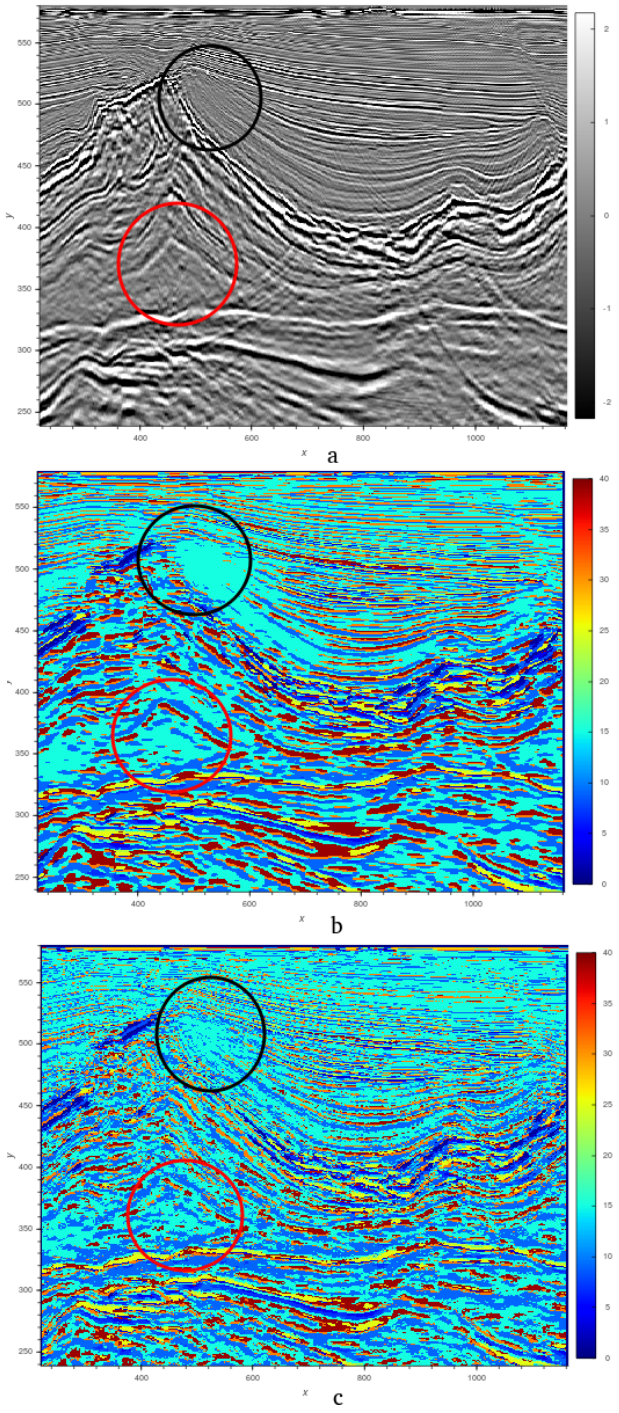

Figure 5: In (a) we see a seismic section image for classification using the cluster labels found; (b) we see the resulting classification using K-Means algorithm; (c) we see the resulting classification using cKDTree algorithm.

Discussion and Conclusion

From what we could learn on this work, the Machine Learning technique combined with the right seismic attributes can be applied to improve image and generate a more accurate model to seismic processing in regions where salt stratification is known as a problem. Not only on salt but also on regions of thin laminations where the layers are smaller than the seismic resolution, the correct attributes, in this case RAI and TECVA , can aid to realize features of the subsurface we could not see before.

As a future work, we plan to extend this research to a 3D

dimension data and test other relevant seismic attributes to see if it can improve the image not only on the salt region but also on thinly laminated structures, providing better and more accurate velocity models.

Acknowledgments

We would like to acknowledge the ANP for providing the dataset for this work, the Euclides da Cunha Foundation (FEC) for the scholarship, Schlumberger for the academic license of Petrel software and GISIS for the academic suppport and infrastructure.

References

BADRINARAYANAN, V., KENDALL, A. AND CIPOLLA, R., [2015]. Segnet: A deep convolutional encoder-decoder architecture for image segmentation. arXiv preprint, arXiv:1511.00561.

BENTLEY, J. L., [1975]. "Multidimensional binary search trees used for associative searching". Communications of the ACM. 18 (9): 509. doi:10.1145/361002.361007.

BULHÕES, E. AND AMORIM, W., [2005] – Princípio da Camada Elementar e sua aplicação à Tecnica Volume de Amplitudes (TECVA). Ninth International Congress of the Brazilian Geophysical Society

GOBATTO, F., MAUL, A., FALCÃO, L., TEIXEIRA, L., BOECHAT, J.B., GONZÁLEZ, M. AND GONZÁLEZ, G., [2016]. Refining Velocity Model within the Salt Section in Santos Basin: an Innovative Workflow to include the Existing Stratification.

LONG, J., SHELHAMER, E. AND DARRELL, T., [2015]. Fully convolutional networks for semantic segmentation. In Proceedings of the IEEE conference on computer vision and pattern recognition, 3431-3440. arXiv:1411.4038.

MANEEWONGVATANA S. AND MOUNT D. M., [1999]. It's okay to be skinny, if your friends are fat. 4th Annual CGC Workshop on Computational Geometry.

MAUL, A., CETALE, M., AND GUIZAN, C., [2018] - Few Considerations, warnings and benefits for the E&P industry when incorporating stratifications inside salt sections. Revista Brasileira de Geofísica, Vol. 36(4), 2018 DOI: http://dx.doi.org/10.22564/rbgf.v36i4.1981.

OLIVEIRA, L., FALCÃO, L., MAUL, A., ROSSETO, J., GONZÁLEZ, M. AND GONZÁLEZ, G., [2015]. Geological Velocity Approach in Order to Obtain a Detailed Velocity Model for the Evaporitic Section, Santos Basin.

SCHUBERT, E. AND GERTZ, M., [2017]. Intrinsic t-Stochastic Neighbor Embedding for Visualization and Outlier Detection. SISAP 2017 – 10th International Conference on Similarity Search and Applications. pp. 188–203.

VAN DER MAATEN, L.J.P. AND HINTON, G.E., [2008]. Visualizing Data Using t-SNE . Journal of Machine Learning Research. 9: 2579–2605.

WALDELAND, A.U., JENSEN, A.C., GELIUS, L.J. AND SOLBERG, A.H.S., [2018]. Convolutional neural networks for automated seismic interpretation. The Leading Edge, 37(7), 529-537.

YAMAMOTO, T., MAUL, A., MARTINI, A., BORN, E. AND GONZALEZ, M., [2017]. Evaporitic Section Characterization Using Inversion and Bayesian Classification

YANG PO, GORDON C., FENG D., VALERIU C., DAVID W., BAOQUAN L., JOS BTM, ROERDINK AND ZHIKUN D., [2016] - GSWO: A programming model for GPU-enabled parallelization of sliding window operations in image processing. Signal Processing: Image Communication Volume 47, September 2016, Pages 332-345